Applied Catalysis B: Environmental 163 (2015) 499–509

Contents lists available at ScienceDirect

Applied Catalysis B: Environmental

journal homepage: www.elsevier.com/locate/apcatb

Aging, re-dispersion, and catalytic oxidation characteristics of model Pd/Al_2O_3 automotive three-way catalysts

Xiaoyin Chen [a], Yisun Cheng [b], Chang Yup Seo [a], Johannes W. Schwank [a,*], Robert W. McCabe [b,**]

[a] University of Michigan, Department of Chemical Engineering, 2300 Hayward, Ann Arbor, MI 48109, USA
[b] Ford Motor Company, Research and Innovation Center, 2101 Village Road, Dearborn, MI 48121, USA

ARTICLE INFO

Article history:
Received 24 February 2014
Received in revised form 1 August 2014
Accepted 8 August 2014
Available online 17 August 2014

Keywords:
Pd/Al_2O_3
TWC
Aging
Re-dispersion
CO and C_3H_6

ABSTRACT

Thermal aging characteristics of model automotive Pd/Al_2O_3 catalyst materials were examined under simulated aging and light-off conditions as a function of aging temperature (up to 1000 °C) in both reducing and oxidizing gas mixtures, and in the presence and absence of steam. The catalysts were characterized by static H_2 chemisorption, thermogravimetric analysis (TGA), powder X-ray diffraction (XRD), and both CO as well as propylene light-off experiments. Aging-induced changes in the Al_2O_3 support were modest and limited to slight loss of BET area and transition from predominantly γ-phase (as received) to θ-phase (after 1000 °C aging). The main deactivation mode of aging was loss of Pd surface area via metallic Pd sintering, especially above the PdO decomposition temperature, as evidenced by higher light-off temperatures. Aging gas composition also impacted the Pd particle size, with more pronounced growth in rich gas (H_2) mixtures. In contrast, particle growth was minimal in lean (O_2) gas mixtures below the PdO decomposition temperature, and sintered Pd particles could be modestly re-dispersed by treating below the PdO decomposition temperatures in O_2 and in the absence of steam. The study suggests strategies for operating vehicles in ways that mitigate or reverse aging effects related to Pd particle growth.

1. Introduction

Palladium (Pd) is the primary oxidation component in most automotive three-way catalysts (TWCs) [1]. To meet stringent emission control requirements over the life of the vehicle, TWCs are typically placed in a close-coupled location near the exhaust manifold outlet to quickly achieve light-off after cold start. This position can result in occasional temperature excursions to 1000 °C or higher during warmed-up engine conditions. Such harsh operating conditions (fuel-rich or lean exhaust containing 10–15% steam) lead to inevitable deactivation of TWCs by a variety of mechanisms that may include thermal deactivation by metal particle growth [2,3], adverse metal–support interactions [4], and even collapse of supporting phases with concomitant encapsulation of metal particles [5–7].

In the past decades, extensive efforts have been made to study aging-induced deactivation of platinum-group metals in TWCs [8,9]. As early as in 1970s, two models were developed for the aging growth kinetics and size distribution of Al_2O_3-supported Pt crystallites to explain the influences of the temperature and reaction atmosphere [10–13]. It was found that the sintering of Pt differs in reducing and oxidizing environments [14,15]. Several publications have addressed Pt sintering and re-dispersion [14–20] under reducing and/or oxidizing conditions. Probably due to the different preparation methods, results for the effect of different atmospheres on the sintering of Pt/Al_2O_3 catalysts have been controversial [14,15,21,22]. Depending on temperature, atmosphere, and metal particle size [14,15], two different mechanisms of Pt particle growth, i.e. crystallite migration [15,18] and atomic or molecular migration (also known as Ostwald ripening) [12,16,19], have been proposed to account for the experimental observations. Similar studies have followed on Al_2O_3-supported Pd catalysts [23], especially for the effects of aging conditions on CO and HC oxidation [2,4,9,24]. It was found that aging characteristics of both Pd and the Al_2O_3 support influence the oxidation activity [25,26]. However, inconsistent results have been reported for the influence of aging atmosphere on catalytic activity [9,27]. While it is generally accepted that Pd sinters more severely in reducing (i.e. rich) atmospheres than in oxidizing (i.e. lean) atmospheres [28], post-treatment of aged TWCs in an oxygen atmosphere has been

* Corresponding author. Tel.: +1 734 764 3374.
** Corresponding author. Tel.: +1 313 337 8042.
E-mail addresses: schwank@umich.edu (J.W. Schwank), rmccabe@ford.com (R.W. McCabe).

http://dx.doi.org/10.1016/j.apcatb.2014.08.018
0926-3373/

shown to improve both the CO and HC oxidation activities due to the improvement of dispersion [29]. An increase of catalytic activity of CH_4 oxidation was also reported after a Pd/Al_2O_3 catalyst was aged in the reactant mixture [30]. In other cases, however, catalysts aged under rich conditions have shown higher activity than those aged under lean conditions [7,24]. Nevertheless, it is still not entirely elucidated whether the mechanism of Pd aging in lean or rich environments follows crystallite migration [23] or sintering via Ostwald ripening [31,32], although a recent in situ TEM study shows that Ostwald ripening dominates the sintering processes associated with loss of Pd surface area and corresponding catalytic activity [32]. While Ostwald ripening may be the dominant coarsening mechanism for metallic Pd particles, it may be difficult to reconcile Pd re-dispersion in an oxidizing atmosphere as the overall Pd particle growth process is complicated by the wide range of (lean and rich) conditions encountered in automotive exhaust. These conditions provide opportunities for vapor-phase transport of Pd at very high-temperatures as well as the potential for encapsulation of Pd particles by the support. In addition, inter-conversion of Pd between metallic and oxide forms, in response to perturbations in the exhaust lambda-ratio, also can be expected to affect Pd particle coarsening and re-dispersion. Given these factors, the overall evolution of Pd particle distributions in TWCs as a function of time-in-use is unlikely to be described by any single particle growth mechanism.

In the case of automotive three-way catalysts, standard development practice involves focusing only on the high-mileage performance (i.e. "full useful life" activity) as achieved in accelerated dynamometer aging protocols. As a consequence, little attention has been directed toward understanding the processes by which catalysts evolve from the fresh to aged states [7,33]; nor has there been much effort to correlate aging characteristics with specific driving conditions [2,4]. Thus, the present study was undertaken to gain deeper insight into the mechanisms by which TWCs age, and assess the impact of several exhaust gas characteristics, namely, temperature, rich or lean gas composition, and the presence or absence of steam. Automotive TWCs are a complex technology, with the HC and CO oxidation functions relying primarily on Pd deposited on alumina- and ceria-containing support phases, often within the same washcoat layer. Thus, we have begun our investigation of TWC aging by breaking this complex catalyst technology into one of its major components, Pd-on-alumina, and focusing on its changes in structure and activity (CO and HC oxidation) as a function of aging conditions. The study reveals that Pd particle coarsening is the primary aging mechanism of Pd/Al_2O_3 under simulated exhaust conditions, and is influenced primarily by temperature but also by exhaust gas stoichiometry (i.e. lean vs. rich) and steam. As such, the results suggest ways of operating the vehicle so as to both inhibit Pd particle coarsening and re-disperse Pd particles before growth becomes extreme.

2. Experimental

2.1. Catalyst preparation

Four Pd/Al_2O_3 model catalysts, having different Pd loadings (0.7–1.6 wt%) and initial Pd dispersions (6.2–16.5%), were prepared by incipient wetness impregnation of SASOL Puralox TH 100/150 Al_2O_3 (BET = 146 m^2/g) with palladium nitrate from aqueous solution. Table 1 summarizes the properties of these fresh catalysts (calcined in air at 500 °C). Samples A and B had roughly the same Pd loading, but differed in the details of their preparation so that sample A had half the dispersion of sample B. Sample C was loaded at half the loading of the other samples. Sample D was prepared on the same SASOL alumina that had been pre-calcined in a muffle furnace in air at 1150 °C for 8 h to significantly lower its surface area (see S-Fig. 1).

Table 1
Initial BET surface area of Al_2O_3, loading and dispersion of Pd on Al_2O_3.

	Sample A	Sample B	Sample C	Sample D
Al_2O_3 support				
BET ($m^2\ g^{-1}$)	146	146	146	66
Pore volume ($cm^3\ g^{-1}$)	1.055	1.055	1.055	0.556
Pd/Al_2O_3				
Pd loading (wt%)	1.6	1.4	0.7	1.4
BET ($m^2\ g^{-1}$)	144	144	127	68
Pore volume ($cm^3\ g^{-1}$)	0.782	1.034	0.832	0.515
Dispersion (%)[a]	8.5	16.5	15.3	6.2

[a] Obtained from H_2 chemisorption at 35 °C.

2.2. Aging protocols

Various aging protocols were employed on Al_2O_3 and Pd/Al_2O_3 catalysts in the absence and in the presence of steam (10%H_2O) at 550 °C, 700 °C, 850 °C, 1000 °C, and 1150 °C, respectively, spanning the range of interest for TWC aging and alumina phase transformation. The Pd/Al_2O_3 catalysts (40–80 mesh size) were held in a quartz tube reactor placed vertically in a clamshell furnace. For aging in the presence of steam (H_2O), the sample was aged for 8 h in either a lean (10%H_2O-16%O_2-10%CO_2-N_2) or rich (10%H_2O-1%H_2-8%CO_2-N_2) flowing gas atmosphere at 550 °C, 700 °C, 850 °C, and 1000 °C, respectively. After aging, the H_2O feed was terminated and the sample was maintained at the same temperature for 20 min in a dry feed prior to cooling the furnace down to room temperature under the same (i.e. dry) feed. For comparison purposes, two separate dry aging protocols were also performed in the absence of H_2O: (1) aging in the same furnace for 8 h but in a dry lean or a dry rich feed; (2) calcination in a muffle furnace for 8 h in a static-air atmosphere.

2.3. Characterization of the alumina and Pd/Al_2O_3 catalysts

Alumina and Pd/Al_2O_3 model catalysts were subjected to an iterative characterization protocol at various stages of aging. N_2 physisorption was carried out at liquid nitrogen temperature on a Micromeritics ASAP 2020 instrument for the characterization of BET specific surface area (SA) and pore volume. In situ XRD experiments for measuring the re-oxidation degree of reduced Pd were carried out with a Scintag X1 diffractometer equipped with an Inel CPS-120 120° 2θ position-sensitive detector using Cu Kα radiation. The sample chamber of the X1 diffractometer was modified with an Edmund Buhler HDK 2.4 environmental chamber containing a resistively heated Fecralloy heating strip. The powder samples were spread onto 0.26 mm thick single-crystal SiC substrates placed directly on top of the heating strip. During patterns scanning, the sample was reduced at 350 °C by a 5%H_2/N_2 flow for 1 h and then purged by a pure N_2 flow prior to exposing to flowing 10%O_2/N_2 at a desired temperature. Ex situ XRD patterns were recorded on a Rigaku rotary anode instrument using CuKα radiation at 40 kV and 100 mA. Thermogravimetric analysis (TGA) of PdO decomposition and Pd re-oxidation was carried out in the presence of flowing 10%O_2/N_2 gas in a TA Q500 instrument at a 2 °C/min ramp rate. The amount of Pd participating in such decomposition–reoxidation cycles was quantified to identify the amount of Pd accessible by oxygen.

H_2 chemisorption experiments were performed on a Micromeritics ASAP 2020 system by means of an adsorption/outgassing/readsorption procedure at 35 °C combined with a 5-point isotherm method extrapolated to zero pressure. A more detailed description of our experimental approach can be found in the supplemental materials (S-Fig.1). Using the uptake

of irreversibly chemisorbed H_2 (S-Fig.2) the Pd dispersion can be calculated by assuming an adsorption stoichiometry of one hydrogen atom per surface palladium atom. The mean Pd particle size or average crystallite size (D) can also be calculated accordingly using a sphere model. The use of H_2 chemisorption for measuring Pd dispersion has been a source of contention in the literature [34] mainly due to concerns about the influence of Pd-hydride formation. To address this concern, an STEM analysis was made for fresh and aged Pd/Al_2O_3 catalyst samples. The Pd particle sizes estimated by H_2 chemisorption were in good agreement with the surface-average particle sizes obtained from electron microscopy.

High angle annular dark field (HAADF) scanning transmission electron microscopy (STEM) images were taken with a JEOL 2010F analytical electron microscope. The microscope, which is equipped with a zirconated tungsten (1 0 0) thermal field emission filament, was operated at 1.5×10^{-7} Torr vacuum with 200 kV accelerating voltage. HAADF STEM images were collected with a JEOL HAADF detector at probe size of 0.5 nm and camera length of 12 cm. Physically crushed catalyst powder was dispersed in ethanol and ultrasonicated for no longer than 10 min prior to mounting onto a 200-mesh carbon coated copper grid. ImageJ software was used for STEM image processing and calculation of the area of single Pd particles. The diameter was estimated with an assumption that each palladium particle is a sphere and the STEM surface-average particle size ($d_p = \sum n_i d_i^3 / \sum n_i d_i^2$) was used for comparison with that obtained by H_2 chemisorption.

2.4. Light-off evaluation of CO and hydrocarbon oxidation

Carbon monoxide (CO) and propylene (C_3H_6) oxidation runs were carried out in an 11 mm diameter quartz tube flow reactor at a ramp rate of 4 °C/min. The Pd/Al_2O_3 catalysts (0.50 g) were diluted by silica gel (1.50 g, Sigma–Aldrich, calcined at 1000 °C for 8 h). The catalyst temperature was controlled by a thermocouple located upstream on the top of the catalyst bed. The gas stream contained 2.50% CO or 0.15% propylene (balanced with N_2) with O_2 adjusted to give the desired lambda value as measured by a Horiba MEXA AFR analyzer. The carrier flow contained 10%H_2O and 10%CO_2 with balance N_2 at a flow rate corresponding to a volumetric space velocity of 50,000 h^{-1}. An MKS FTIR spectrometer was used for the analysis of reactant and product gas components (CO, C_3H_6, CO_2, and H_2O). It should be pointed out that recent work in our laboratory has shown that similarly prepared Pd/Al_2O_3 catalysts demonstrate less than 4% CO conversion in WGS up to 350 °C even in the fresh state. The low WGS activity of these catalysts is not surprising given that the adsorption and dissociation of H_2O on Pd is highly non-competitive with CO adsorption under low-temperature and net oxidative (i.e. light-off at lambda >1.0) conditions.

3. Results and discussion

3.1. Effects of lean and rich aging on Pd dispersion

Table 1 compares the properties of the blank Al_2O_3 and the Pd/Al_2O_3 catalysts. SASOL TH 100/150 Al_2O_3 is a high-pore-volume thermally stable alumina with nominal 10 nm median pore radius and 150 m^2/g BET surface area. Our measured values of 146 m^2/g surface area and 1.055 cm^3/g pore volume for the 500 °C calcined alumina (samples A, B, C) are consistent with the nominal values reported by SASOL. Even after calcination at 1150 °C for 8 h, the BET surface area and the pore volume still remain high at 66 m^2/g and 0.556 cm^3/g, respectively. The 500 °C calcined TH 100/150 is γ-phase, while the 1150 °C calcined material is mostly a mix of θ and α phases (S-Fig. 3). The loading of Pd (0.7–1.6 wt%) has only a slight influence on the surface area of Al_2O_3. But, depending on the impregnation method, the decrease of pore volume was obvious in samples A and C. The Pd particle size estimated from H_2 chemisorption for sample B (16.5%) is 6.8 nm, in good agreement with the 7.2 nm obtained from STEM surface-average, as shown in Fig. 1(a).

Table 2 lists the effects of aging temperature and environment on Pd dispersion of the Pd/Al_2O_3 catalysts. For all of the catalysts and aging temperatures, aging under rich conditions sintered the Pd more severely than under lean conditions. Specifically considering the lean and rich aging conditions separately, all of the samples showed a more pronounced decrease in dispersion with increasing temperature under rich aging conditions. Contrary to what one might expect, higher initial Pd dispersion (comparing A and B), lower Pd loading (comparing B and C), and pre-sintering of Al_2O_3 (comparing B and D) do not appear to contribute to making Pd less susceptible to sintering in the rich environment. In contrast, lean aging, over all four samples, resulted in little change in dispersion between 550 °C and 700 °C, but considering the individual samples during lean aging below 850 °C, sintering of the initially highly dispersed samples B and C was minimal while re-dispersion was observed for the lower dispersion samples A and D. Lean aging produced a sharp reduction in dispersion at 850 °C and 1000 °C. The aging influence on the state of Pd/Al_2O_3 catalysts can also be confirmed by STEM analysis (Fig. 1(a)–(c)) and visual observation (S-Fig 4). Bulk PdO decomposes near 800 °C under the aging conditions employed [35,36], so the sharp decreases in dispersion observed under both lean and rich aging conditions at temperatures of 850 °C and 1000 °C reflect coarsening of metallic particles. The Pd particle size, measured by H_2 chemisorption, increased from 6.8 nm (fresh) to 30.0 nm (850 °C aging in rich condition), compatible with the change of surface-average particle size from 7.2 nm to 18.2 nm, measured by STEM. Such severe sintering resulted in a broad particle size distribution, as shown in Fig. 1(c). While all of the samples showed the same general sintering trends with both temperature and lean versus rich exposure, samples C and D displayed notably different aging characteristics compared to the similarly prepared sample B. The lower-loaded sample C (0.7 wt% Pd) started out with a high initial dispersion close to that of its higher loaded counterpart sample B (1.4 wt% Pd), and maintained a significantly higher dispersion with increasing temperature under lean conditions, yet suffered a greater loss of dispersion under rich conditions. Sample D (prepared on the pre-sintered alumina) started out with lower dispersion than any of the other samples and maintained a lower dispersion at all aging conditions.

3.2. Effect of steam and re-dispersion of PdO

The above results were obtained from Pd/Al_2O_3 catalysts after aging in gas mixtures containing 10%H_2O. For comparison, additional experiments were carried out in the absence of steam. Fig. 2 compares the BET surface areas of the blank Al_2O_3 and the Pd/Al_2O_3 catalysts after aging in the absence of steam (static calcination in dry air) and in the presence of steam (flowing gas mixtures containing 10%H_2O). Considering first the blank Al_2O_3 (open and closed diamonds in Fig. 2), aging in the presence of steam decreases the BET area by about 20 m^2/g over the entire temperature range. Interestingly, this offset does not reflect differences in the phase transformation of the Al_2O_3 with increasing temperature. XRD data (Fig. 3) show essentially identical patterns for the predominantly γ-Al_2O_3 after aging either in the presence or absence of H_2O at 500 °C. Moreover, it can be seen that aging in the presence of H_2O hastens the development of θ-Al_2O_3 features with increasing temperature, but without significant loss of surface area beyond that observed at 500 °C in Fig. 2. In addition, Fig. 2 also shows that aging of the Pd-containing catalysts in the presence of 10%H_2O – either rich or lean – does not produce an incremental loss in BET area over that

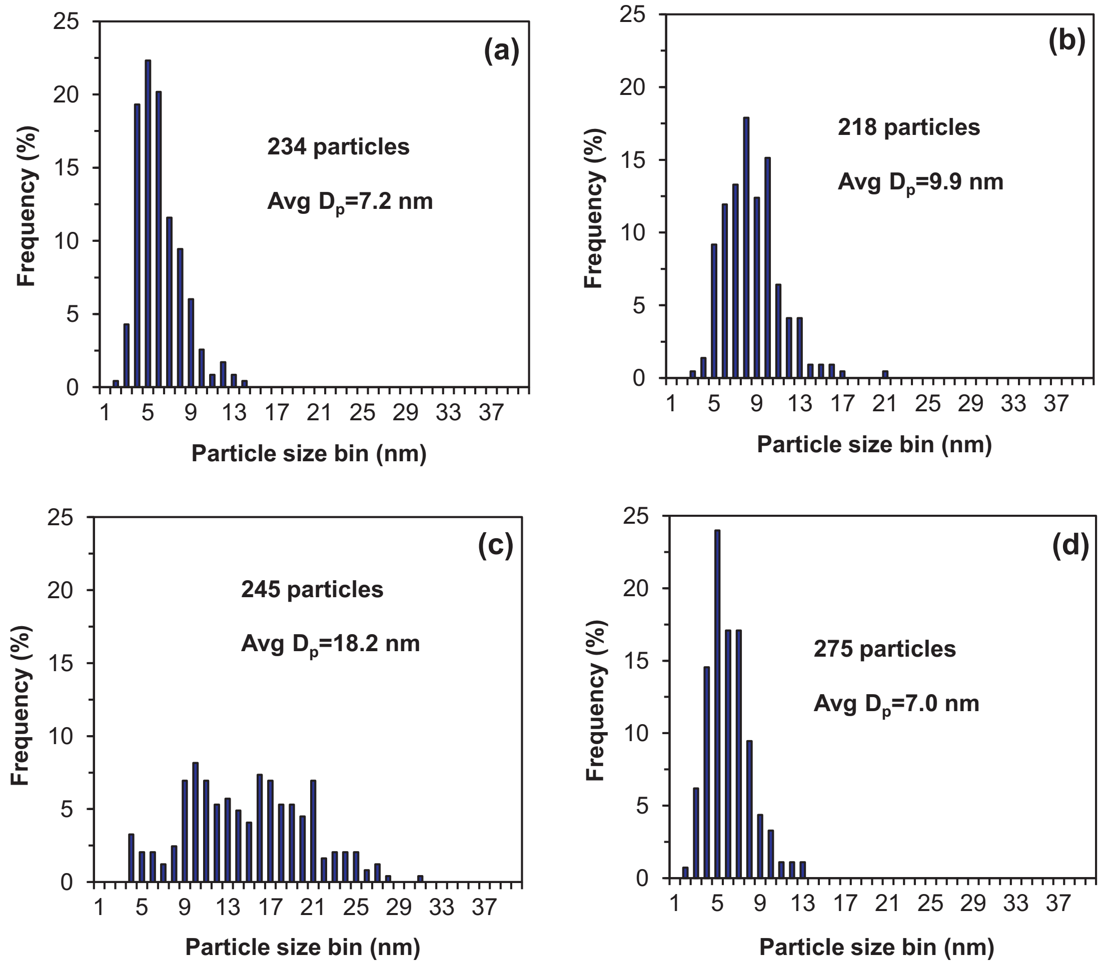

Fig. 1. Pd particle size distribution of sample B measured by STEM: (a) fresh, (b) 700 °C aged in rich condition, (c) 850 °C aged in rich condition, and (d) 700 °C aged in lean condition without steam.

observed with the blank Al_2O_3. These results indicate that neither impregnation of Pd (at the 1.4% level) nor aging in rich versus lean gas environments (in the presence of steam) significantly changes the pore properties of the Al_2O_3.

In addition to the effect of steam on the pore properties of the Al_2O_3 support, we conducted an additional series of aging experiments of selected Pd/Al_2O_3 catalysts at temperatures of 550–850 °C in the same lean or rich flowing conditions but without H_2O in the feed, and subsequently measured the Pd dispersion. The results are listed in Table 3. For all samples, the Pd dispersion post aging in the dry, lean feed is much higher than that post aging in the wet, lean feed (Table 2) at the same temperature. For example for sample B, aging at 550 °C, 700 °C and 850 °C without steam gave Pd dispersions of 19.6, 22.1 and 10.5%, whereas the corresponding values after aging in the presence of steam were 14.4%, 12.7% and 5.2%, respectively. Furthermore, both the 19.6% and 22.1% values for sample B at 550 °C and 700 °C, respectively, are higher than the value of 16.5% obtained for the fresh sample (calcined at 500 °C in air, see Table 1). The re-dispersion of Pd particles is confirmed by STEM analysis, as shown in Fig. 1(d). Also, Pd dispersion post aging at 700 °C (22.1%) is higher than that post aging at 550 °C (19.6%), indicating that the Pd dispersion increases with increasing aging temperature up to 700 °C. When aging was performed at 850 °C in the same dry conditions, the Pd dispersion declined, but the value (10.5%) was still double the value (5.2%) post aging in steam (Table 2), thus indicating a suppression of Pd sintering even above the PdO decomposition temperature in the absence of steam. The latter observation is confirmed by comparing the dispersion data after 1000 °C lean aging between Tables 2 and 3, where aging under dry conditions (static muffle furnace) produced

Table 2
Pd dispersion (%) of samples after aging in steam[a] and re-oxidation.[b]

Aging T (°C)	Sample A			Sample B			Sample C			Sample D		
	L-	R-	Re-oxid[b]	L-	R-	Re-oxid[b]	L-	R-	Re-oxid[b]	L-	R-	Re-oxid[b]
550	9.5	7.6		14.4	7.2	9.3	13.4	7.7		6.3	3.8	
700	10.2	6.1	6.0	12.7	5.8	7.5	13.7	4.1	5.3	6.7	2.7	4.0
850	4.5	3.3		5.2	3.7	4.0	8.9	1.8		3.9	0.9	
1000	2.9	1.3		1.4	0.6		2.7	u/d[c]		1.1	u/d[c]	

[a] L- and R- represent lean and rich aging, respectively.
[b] Re-oxidation was performed by calcination at 550 °C in the muffle furnace for 8 h on rich-aged samples.
[c] u/d represents "undetectable".

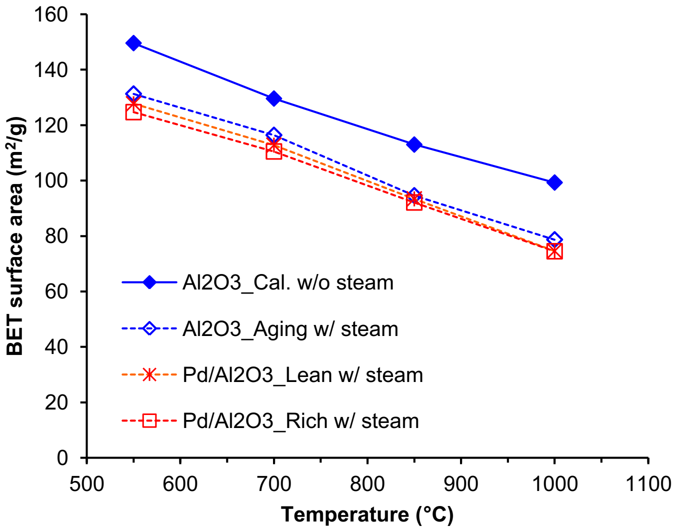

Fig. 2. BET surface areas of Al_2O_3 and Pd/Al_2O_3 (sample B) vs temperature of calcination and aging under different conditions.

Table 3
Pd dispersion (%) of samples aged in absence of steam.[a]

Aging temperature	Sample A		Sample B		Sample C		Sample D	
(°C)	L-	R-	L-	R-	L-	R-	L-	R-
550			19.6	7.8				
700	13.4	5.0	22.1	5.0	20.1	3.8	10.0	2.2
850			10.5					
1000[b]	3.0		3.9				2.1	

[a] L- and R- represent lean and rich aging, respectively.
[b] Aging by calcination at 1000 °C in the muffle furnace.

equal or higher dispersions than aging under wet conditions (flow reactor).

Table 2 also shows dispersion data for selected rich-aged samples that were then re-oxidized in air in a muffle furnace for 8 h at 550 °C. In all but one case, the re-oxidation resulted in a modest increase in dispersion, indicating that sintered Pd particles could be modestly re-dispersed by treating in O_2 and in the absence of steam.

In contrast to the dry lean aging results, aging under dry rich conditions did not result in a higher Pd dispersion for any of the samples investigated. For example, aging at 700 °C in the dry rich feed gave slightly lower Pd dispersions than aging in the same environment with steam for all four-catalyst samples. Finally, it should be noted that in addition to the re-oxidation data for the rich aged catalysts shown in Table 2, several other examples of increased Pd dispersion with oxygen exposure at 700 °C or below can be seen in comparing data between Tables 1–3. Such evidence for Pd re-dispersion can be most clearly seen in samples A and D that started out with lower dispersion as initially calcined at 500 °C. For example as mentioned above, sample A had an initial dispersion of 8.5% but increased to 9.5% (after 550 °C lean/wet aging), 10.2% (after 700 °C lean/wet aging) and 13.4% (after 700 °C lean/dry aging). Summarizing the dispersion results, our data show that the most favorable conditions for achieving and maintaining high Pd dispersion are to expose the catalyst to oxygen at temperatures near (but below) the PdO decomposition temperature in a dry environment.

3.3. *PdO decomposition and Pd re-oxidation*

The sensitivity of the Pd dispersion to lean and rich aging conditions indicates that the Pd oxidation state plays an important role in Pd particle coarsening on Al_2O_3. Moreover, irreversible interaction of Pd with the support and/or encapsulation of Pd by the support represent potential deactivation mechanisms for Pd/Al_2O_3 catalysts in addition to Pd particle coarsening. We have carried out TGA studies to gain insight into the Pd oxide formation and decomposition characteristics of these catalysts and to assess the extent to which support interactions or encapsulation might contribute to aging effects.

Fig. 4 shows typical TG and DTG curves of the 1000 °C rich aged samples B (Fig. 4a) and D (Fig. 4b) after multiple PdO decomposition (increasing temperature) and Pd re-oxidation (decreasing temperature) cycles in flowing 10%O_2/N_2. Table 4 lists the DTG peaks and Pd amounts that participate in the PdO–Pd–PdO cyclic transformation for samples B, D, and bulk PdO powder (Aldrich, 99.999%). During PdO decomposition, O_2 evolution was experimentally confirmed in our work by installing an oxygen sensor downstream of the TGA furnace. The key features of these data are a two-step PdO decomposition profile (with various amounts of the first and second DTG peaks depending on history of the sample, e.g. number of repeated cycles) and only one re-oxidation peak that occurs at a significantly lower temperature than the first portion of oxide decomposition. Bulk PdO powder showed only one decomposition peak in the range of 805–815 °C [36]. The fresh sample B showed in the first couple of heating/cooling cycles one DTG peak (S-Fig. 5) above 860 °C that can most likely be attributed to a contribution from initial dehydration

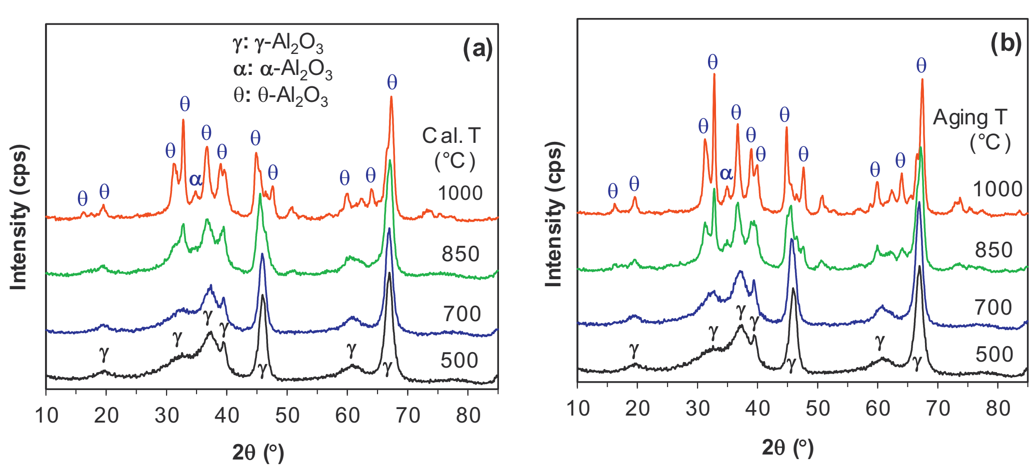

Fig. 3. XRD patterns of Al_2O_3 post calcination without steam (A) and aging with steam (B) under different temperatures. The symbols γ, θ, α represent the peaks of structural phases of Al_2O_3, respectively.

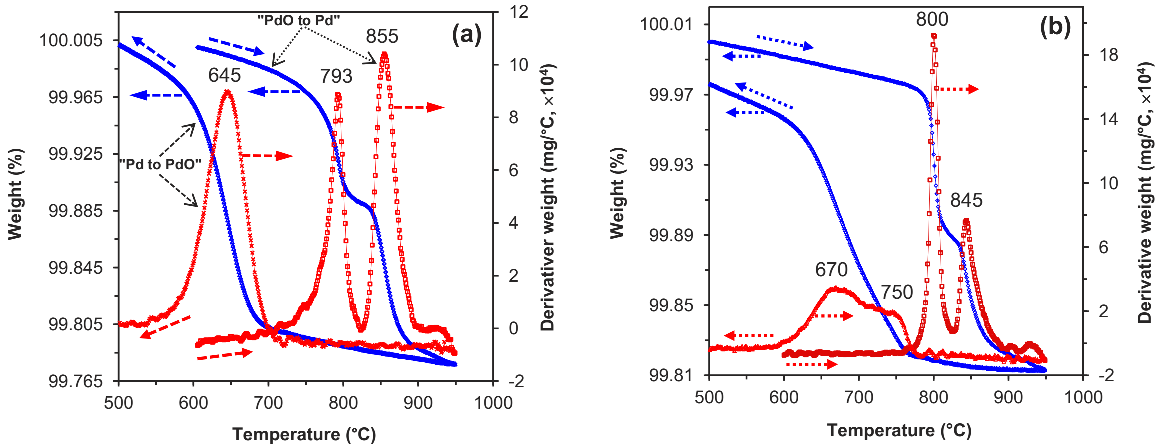

Fig. 4. TG and DTG curves for PdO–Pd–PdO cyclic transformation. (a): repeated cycle, sample B 1000 °C aged in rich condition; (b) 3rd cycle, sample D 1000 °C aged in rich condition.

of the sample. After several cycles, the peak stabilized at around 850 °C and another peak emerged around 800 °C (see Fig. 4a, S-Fig. 5, and Table 4). For the 1000 °C-aged sample B (independent of aging atmosphere), the first cycle gave only one peak at T = 845 °C. The appearance of two PdO decomposition peaks was observed in the 2nd cycle. However, PdO supported on pre-calcined Al_2O_3 (sample D) gave immediately two decomposition peaks in the 1st cycle (S-Fig. 6). The 1st peak at lower temperature stabilized at ~800 °C for all samples, while the 2nd peak, depending on aging and Al_2O_3 structure, stabilized in the range of 840–860 °C (Table 4). A number of studies have been directed toward understanding both the decomposition and re-oxidation features [35–39], with the general consensus that PdO decomposition is thermodynamically controlled and re-oxidation is kinetically limited. Our group has recently carried out a detailed study of PdO decomposition on alumina providing evidence for surface-initiated decomposition of PdO particles near the normal PdO decomposition temperature (1st peak) resulting in formation of a Pd metal shell that inhibits decomposition of the remaining PdO core to temperatures above the bulk thermodynamic decomposition temperature [36]. For the purposes of the present study, however, the main significance of the TGA data is in helping to explain the Pd particle sintering and re-dispersion data observed under lean aging conditions. As noted above, bulk PdO decomposes around 800 °C [36], and the core PdO decomposition rate peaks around 850 °C for PdO on γ-Al_2O_3 (even for PdO in the stabilized Pd-shell/PdO-core structure). Thus, the sharp decrease in Pd dispersion under lean aging conditions in going from 700 °C to 850 °C aging conditions (Tables 2 and 3) is consistent with transformation of the Pd species from PdO to metallic Pd. Re-oxidation begins near 700 °C (or higher depending on the particular sample and its history) and the rate generally peaks around 650 °C (Fig. 4 and Table 4) and then falls to low levels near 500 °C. Thus, all of the data in Tables 2 and 3 showing re-dispersion of Pd involve heating samples in lean conditions at 550 °C or 700 °C where the PdO is stable and oxidation rates are relatively high.

Besides the identification of PdO decomposition and Pd re-oxidation temperatures, TGA can also provide the quantification of weight loss due to PdO decomposition to show what portion of the Pd participates in the PdO–Pd–PdO cyclic transformation and whether Pd is partially encapsulated by Al_2O_3 under aging conditions. For comparison and peak identification, Table 4 also lists the 2nd- and 3rd-cycle weight loss quantification for both the B and D samples after various treatments, and corresponding data for bulk PdO powder. First-cycle data generally show apparent weight loss in excess of the theoretical amount associated with PdO decomposition due to dehydration of the alumina, but the dehydration contribution is minimal after the 1st cycle and the values reported for sample B in Table 4 match (within experimental error) expected values based on all of the Pd participating in the PdO–Pd–PdO transformation. Sample D, however, presents a different picture. All of the Pd is involved in the PdO–Pd–PdO transformation for the fresh catalyst, and only a small amount (5%) of weight is lost in the 1000 °C lean-aged sample, but the 1000 °C rich aged sample shows only about 75% Pd participation. While in principle the

Table 4
TGA peak features and Pd amount (%) participated in PdO–Pd–PdO cyclic transformation.[a]

Sample	Cycle 2				Cycle 3			
	Pd amount[b]		Decomp. peak	Re-oxid. peak	Pd amount[b]		Decomp. peak	Re-oxid. peak
	Total (%)	1st (%)	(°C)	(°C)	Total (%)	1st (%)	(°C)	(°C)
Sample B								
500 °C Cal. (fresh)	110	0	none/883	598	107	22	790/868	602
1000 °C L-aged	102	18	794/856	647	101	21	794/856	647
1000 °C R-aged	107	18	792/860	645	105	21	792/859	645
Sample D								
500 °C Cal. (fresh)	104	38	811/835	550–760[c]	102	40	808/835	550–760[c]
1000 °C L-aged	95	39	804/839	672	91	42	802/839	676
1000 °C R-aged	74	38	800/845	600–780[c]	75	40	800/845	600–780[c]
PdO powder	9	9	807	752	6	6	805	751

[a] Data obtained in the range of temperature at 700–950 °C.
[b] Total and 1st peak contributed Pd amounts (%) that involve in PdO–Pd–PdO cyclic transformation.
[c] A broad re-oxidation peak in the range.

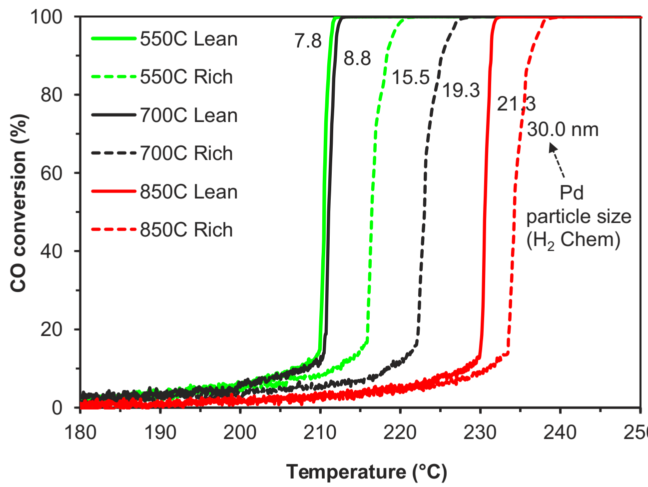

Fig. 5. Effect of aging temperature and environment on CO light-off over Pd/Al_2O_3 catalyst (sample B). The aged catalyst was pre-oxidized at 550 °C for 2 h in $10\%O_2$ flow prior to CO oxidation with lambda of 1.01.

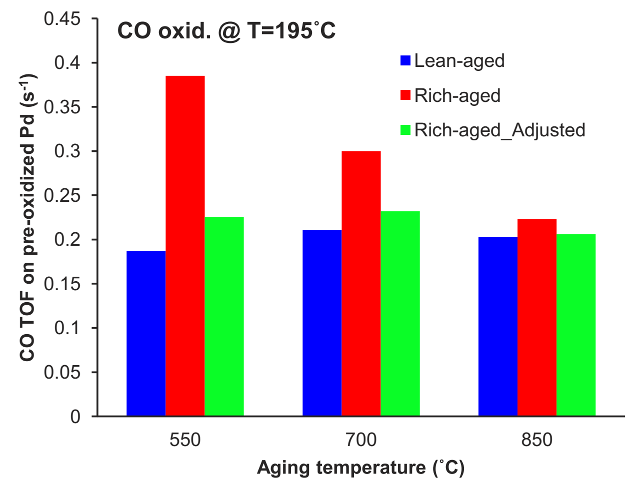

Fig. 7. CO TOF comparison of lean- and rich-aged Pd/Al_2O_3 catalysts (sample B). CO TOF was obtained from CO conversion and Pd particle size shown in Fig. 5.

weight loss could be due to Pd encapsulation by the support, a more likely scenario is suggested by similarities between the traces shown in Fig. 4b and those of bulk PdO powder [36]. Pd encapsulation by Al_2O_3 is unlikely, as for sample D the Al_2O_3 support was pre-sintered at 1150 °C prior to loading of Pd. 1150 °C pre-treatment leads to formation of a mixture containing strong α and θ phases (S-Fig. 3), while 1000 °C rich-aging mainly made a phase transformation from γ to θ. The bulk PdO powder exhibits only one decomposition peak that is narrow and commensurate in temperature with the 1st peak in Fig. 4b. Moreover, the bulk PdO powder showed 100% decomposition in the 1st cycle, but only 9% and 6% of Pd participates in the PdO to Pd transformation in the 2nd and 3rd cycles, respectively, indicating a kinetic limitation on re-oxidizing the large (order 1 μm) Pd particles. We suspect that the Pd particle coarsening is so severe for the 1000 °C rich aged Pd on the pre-sintered alumina support (dispersion undetectable – Table 2) that a portion of the Pd particles has taken on bulk Pd/PdO characteristics [36].

3.4. Oxidation light-offs over Pd/Al_2O_3

CO and propylene light-off runs were carried out to assess the effects of the various aging and pre-treatment conditions on catalytic activity. Fig. 5 shows CO light-off curves over sample B after aging under the lean and rich conditions shown in Table 2. To better compare the activity, the samples were all treated (pre-oxidized) for 2 h at 550 °C in a dry $10\%O_2/N_2$ flow prior to reaction. The values listed next to the CO light-off curves represent the Pd particle size measured post aging. The trends in light-off temperature of CO oxidation reflect the trends in Pd dispersion, i.e. lower Pd dispersions result in higher CO light-off temperatures. Also, as apparent in Table 2, the observed dispersions reflect a combination of thermal and gas environment effects that combine to give the following sequence of light-off temperatures: 550 °C lean < 700 °C lean < 550 °C rich < 700 °C rich < 850 °C lean < 850 °C rich.

In addition to the primary effects of aging temperature and rich- or lean-aging environment on CO oxidation light-off, the oxidizing pre-treatment employed prior to the light-off experiments of Fig. 5 changes the oxidation state of the Pd and increases the Pd dispersion relative to the state immediately post aging, particularly for the post rich-aging samples. To explore this possibility, CO light-off of the as-aged samples was examined after a pre-reducing treatment for 2 h at 350 °C in a dry 1% H_2 flow. For comparison purposes, the data of Fig. 5 for the pre-oxidized samples are reproduced in Fig. 6 along with the corresponding data for the pre-reduced samples. Without exception, the light-off temperature is lower for the lean pre-treated samples than for the corresponding rich pre-treated samples, as shown for both the rich aged (Fig. 6a) and lean aged (Fig. 6b) samples regardless of aging temperature. To further reveal the effect of aging environment on catalytic activity, Fig. 7 shows CO TOF (at 195 °C) over the pre-oxidized lean- and rich-aged Pd/Al_2O_3 catalysts. Catalysts post lean aging at 550, 700, and 850 °C had very similar TOFs in the range of 0.19–0.21 s^{-1}. Post rich aging,

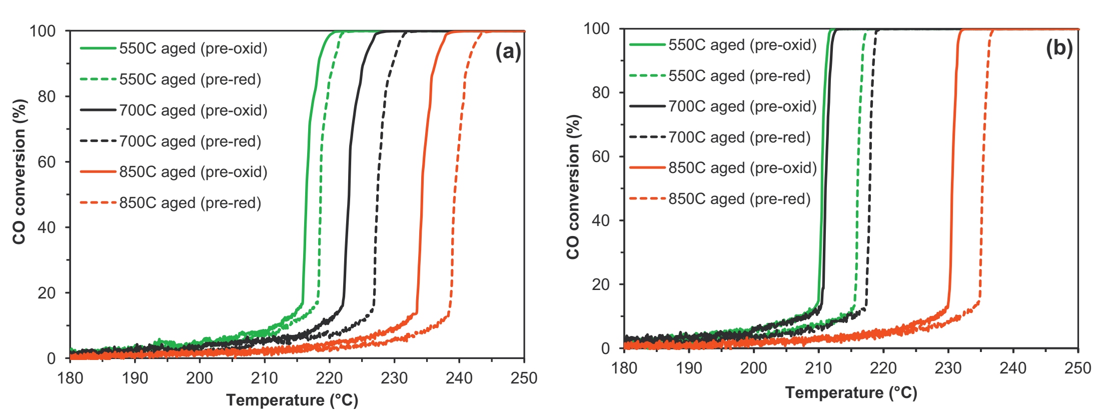

Fig. 6. Effect of pre-treatment environment on CO oxidation (lambda = 1.01) over Pd/Al_2O_3 catalyst (sample B) aged in rich (a) or in lean (b) condition. The pre-treatment of Pd/Al_2O_3 catalyst was performed at 550 °C in $10\%O_2$ flow (solid line) or at 350 °C in $1\%H_2/N_2$ flow (dash line) prior to CO oxidation.

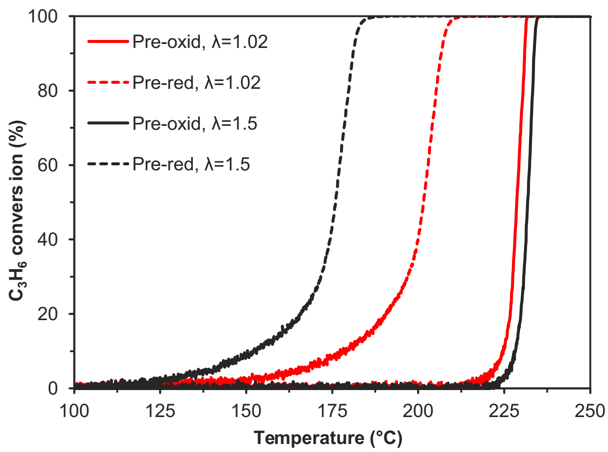

Fig. 8. Light-off curves of C_3H_6 oxidation over Pd/Al_2O_3 (sample B), which was rich-aged at 850 °C for 8 h and then pre-treated in the reducing (dash line) or oxidizing (solid line) flows prior to C_3H_6 oxidation.

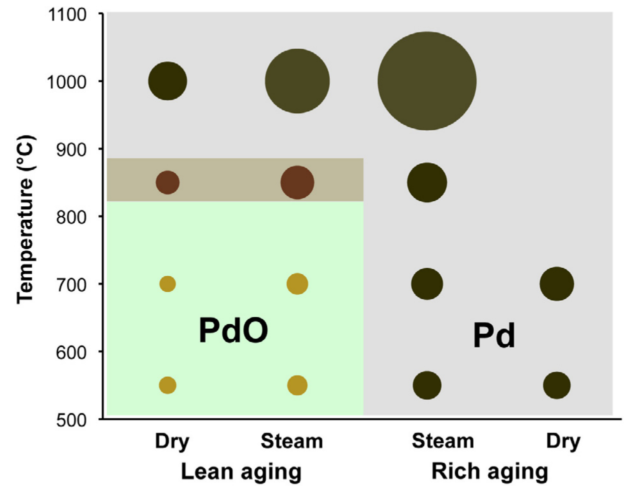

Fig. 9. Schematic depiction of effect of aging conditions and temperature on particles size of Pd species for sample B (symbolized by the proportional size of spheres). The band surrounding the 850 °C point represents the transition regime from PdO to Pd.

however, TOFs in the range of 0.22–0.39 s^{-1} were obtained for the corresponding temperatures. Having considered the re-dispersing effect of pre-oxidizing on the rich-aged Pd/Al_2O_3 (Table 2), these TOFs were adjusted to reflect the extent of re-dispersion (Fig. 7). The dispersion-adjusted TOFs over the rich-aged samples became nearly identical to those over the lean-aged catalysts within the experimental error. The results are consistent with the structure insensitive nature of the CO oxidation over Pd/Al_2O_3 [40,41].

To gain additional insights into the oxidation characteristics of Pd/Al_2O_3, C_3H_6 oxidation was also performed over the pre-oxidized and pre-reduced 850 °C rich-aged Pd/Al_2O_3 (sample B) under different λ conditions. The C_3H_6 conversion vs. temperature is shown in Fig. 8. In contrast to CO oxidation, the pre-reduced catalyst gave dramatically lower light-off temperatures than the pre-oxidized one at both λ levels, although pre-oxidation prior to reaction can modestly re-disperse the sintered Pd particles. At higher oxygen concentration (with λ increased from 1.02 to 1.50), the gap widened by shifting the light-off temperature substantially lower for the pre-reduced catalyst and slightly higher for the pre-oxidized catalyst. The lower C_3H_6 light-off temperatures of pre-reduced catalysts compared to those of pre-oxidized samples were confirmed over both 700 °C lean- and rich-aged samples, and the gap also widened when higher λ conditions were applied. For example, for the 700 °C lean-aged Pd/Al_2O_3 catalyst (sample B), the $T_{50\%}$ of pre-reduced and pre-oxidized samples was 214 °C and 223 °C for $\lambda = 1.01$, whereas these values were 181 °C and 223 °C, respectively, for $\lambda = 1.4$.

3.5. Discussion

3.5.1. Pd sintering

Retention of relatively high alumina surface area (75 m^2/g at the 1000 °C aging temperature) combined with TGA data showing no loss of accessible Pd, and STEM evidence of relatively large Pd particles showing little wetting of the alumina support [36], all indicate that the deactivation of Pd/Al_2O_3 catalysts under the aging conditions of our study does not involve either encapsulation of Pd or irreversible interactions between Pd and the alumina. Instead, the dramatic loss of H_2 chemisorption capacity (combined with corresponding STEM data showing 60–80 nm Pd particles after 1000 °C rich aging in our companion study [36]) indicates that Pd particle coarsening is the main deactivation mode of a model Pd/Al_2O_3 three-way catalyst component. The Pd particle coarsening and attendant effects on CO and C_3H_6 light-off activity depend primarily on aging temperature and environment (i.e. rich or lean gas mixture), and also on the presence of steam if aging is carried out under lean conditions. Correlation of the light-off activity data to aging conditions is further complicated by changes in the Pd (or PdO) particles that occur post aging related to factors such as the gas environment experienced during cool-down, the pre-treatment utilized prior to activity testing, and also the lambda-value at which the catalysts are evaluated.

Most of the results of the present study can be explained by considering the state of the Pd – i.e. Pd metal or PdO – after each aging treatment. Conditions that promote Pd oxidation preserve (and in some cases increase) Pd dispersion [42]. This can be clearly seen in Table 2 where the 550 and 700 °C lean aging conditions resulted in only a small loss of Pd dispersion compared to the fresh (500 °C calcined samples). In contrast, all of the rich aging conditions and lean aging at temperatures above the bulk PdO decomposition temperature (ca 800 °C) resulted in continuous and dramatic decreases in Pd particle dispersion with increasing temperature. This can be clearly illustrated by Fig. 9 that schematically shows for sample B the influence of aging environment (rich versus lean, dry versus wet). The trends in dispersion are reflected in the CO light-off curves of Fig. 5 where the 550 °C and 700 °C lean aging (i.e. stable PdO) resulted in the lowest light-off temperatures, followed at successively higher temperatures by the 550 °C rich aged, 700 °C rich aged, 850 °C lean aged and 850 °C rich aged samples – all composed of metallic Pd particles following their respective aging conditions.

In addition to the trend of increasing CO light-off temperature with decreasing dispersion, Table 2 and Fig. 5 also show that dispersion is greater and light-off temperature is lower for the lean aged catalyst at each aging temperature. Interestingly, this holds even for the 850 °C aged catalyst where Pd is the stable phase in both cases. We cannot rule out the possibility that the presence of gaseous oxygen mitigates Pd particle growth to some extent even above the PdO decomposition temperature, but a more likely scenario is that part of the sintered metallic Pd is re-dispersed as the sample is slowly cooled in the lean feed following the lean aging (whereas the rich aged sample is cooled in the same rich feed). As shown in Fig. 4, cool-down of metallic Pd from 950 °C in a lean feed traverses the temperature range where Pd oxidation is most rapid.

In addition to the primary aging effects of temperature and gas environment, the data of Fig. 6, showing lower light-off temperatures for the lean vs rich pre-treated samples, indicate that CO light-off is favored on oxidized Pd particles. This observation is consistent with several recent studies suggesting (via spectroscopic

and/or kinetic analysis) that oxidized Pd surfaces are more active than metallic Pd for CO light-off [43–46]. However, the 550 °C lean pre-treatment also has the potential to re-disperse the rich aged samples to some extent as shown in Table 2 for the B samples used in the CO light-off experiments. As Table 3 shows, the Pd particles in the fresh samples could further re-disperse during aging in a dry and lean condition at temperatures below the PdO decomposition temperature. Furthermore, the results from Maillet et al. [47] showed that the reduction of pre-oxidized PdO in the sintered Pd/γ-Al_2O_3 catalyst occurs at $T < 184$ °C, that is before CO oxidation starts. Thus, the lower light-off temperatures observed for the pre-oxidized samples may represent the combined effects of a chemically more reactive surface (due to oxidation) and a greater site density (due to re-dispersion) [29].

In contrast to CO oxidation, light-off in C_3H_6 oxidation is favored on the pre-reduced catalyst and occurs at lower temperatures. The higher activity on the pre-reduced surface is consistent with the fact that the propylene sticking coefficient on Pd is a factor 5 higher than on the PdO surface [48] although once propylene adsorbs, the PdO monolayer catalyzes its oxidation at lower temperatures than metallic Pd and the C—H bond cleavage of propylene is highly facile on the PdO surface to favor the deep oxidation [49]. We also observed that increasing the oxygen concentration decreased the light-off temperature on the pre-reduced surface but had no significant effect on the pre-oxidized surface (Fig. 8). Our C_3H_6 light-off results were confirmed on both rich and lean-aged catalysts and agree with previous observations [50] for C_3H_6 oxidation over a Pd-only monolithic catalyst that was initially reduced in rich exhaust and then evaluated on lean temperature ramps. It is important to remember that going from a pre-reduced to a pre-oxidized surface also changes the particle size, and this could have some ramifications for adsorption and reactivity. For example, a size effect was invoked to explain why the specific oxidation rates of propylene over Pd/Al_2O_3 catalyst were at least one order of magnitude lower than over Pd wire [51]. Another evidence is the di-σ-molecules preferentially adsorbed on the larger Pd particles [52]. Given the complexity of propylene adsorption and reaction on Pd, our data set is not large enough to address the question of structure sensitivity of propylene oxidation.

The final factor we have investigated relative to Pd/Al_2O_3 deactivation is the presence or absence of water vapor (steam) under aging conditions. The presence of steam causes a small surface area loss in the blank alumina that is observed at the lowest aging temperature and persists in magnitude up to the highest aging temperatures. Addition of Pd to the catalyst, combined with aging under either lean or rich conditions does not significantly affect the surface area loss relative to the blank alumina. In contrast, the Pd particle dispersion depends strongly on the presence or absence of steam, but only under the lean aging condition. The acceleration of Pt sintering on γ-Al_2O_3 was observed in the presence of steam during an oxidizing treatment at 550 °C [9] and it was also reported that palladium sintered more rapidly in a steam atmosphere than in vacuum or hydrogen [53]. Several catalyst-aging studies have associated particle growth with the presence of hydroxyl species on the surface of alumina [54–56]. We thus speculate that aging under the relatively high temperatures of our study in the absence of steam results in a highly dehydrated surface with a high density of defect sites capable of anchoring PdO particles and mitigating particle growth. The addition of oxygen in the absence of steam would not be expected to affect the defect density associated with missing hydroxyl groups. However, addition of hydrogen in the absence of steam has the potential to partly re-hydroxylate the alumina (especially in the vicinity of Pd metal particles that can dissociate H_2 and promote spillover to the alumina). Thus, the observed dispersion data are consistent with a steam effect (i.e. sintering promoted by alumina surface hydroxyl groups) occurring in a rich hydrogen-containing gas regardless of the presence or absence of H_2O vapor, but occurring in a lean oxygen-containing gas only in the presence of steam.

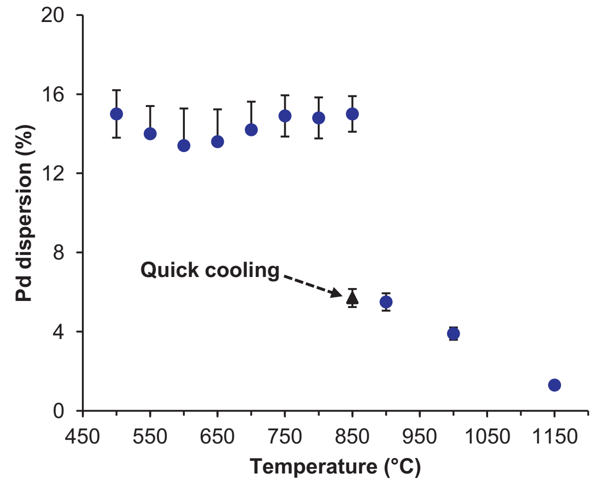

Fig. 10. Pd dispersions of fresh Pd/Al_2O_3 (sample B) after re-calcination at the indicated temperatures for 8 h followed by slow cooling to room temperature in static-air in a muffle furnace; (▲) represents the result obtained when an 850 °C re-calcined sample is instead quickly cooled in ambient air.

3.5.2. Arrested Pd sintering and Pd re-dispersion: implications for automotive TWCs

The data of Table 2 show that modest re-dispersion of rich aged Pd samples can be affected by re-oxidizing for 8 h at 550 °C. The increases in dispersion are of the magnitude expected from the volume change and partial fracturing and roughening of the particle surface associated with conversion of Pd to PdO [36]. Hence, our data show no evidence for complete break-up and oxidation of large Pd particles into smaller PdO particles accompanied by large-scale migration over the Al_2O_3 surface. In contrast, the dispersion of lean aged samples can be seen in Table 2 to remain high and even higher than fresh levels (Table 3) up to the PdO decomposition temperatures. This trend can be seen more clearly in Fig. 10 for the fresh (sample B) catalyst aged for 8 h in air in a muffle furnace followed by slow cooling inside the muffle furnace (solid circles). Interestingly, the starting dispersion could be maintained up to 850 °C (i.e. above the bulk PdO to Pd transformation temperature of 817 °C [36]) when natural slow cooling was performed. But when the sample was ballistically cooled by removing it from the furnace and exposing it to ambient air, the Pd dispersion decreased to a level closer to the dispersion levels observed for rich aged samples. We suspect that this quick cooling process, where the temperature dropped quickly below that where Pd can oxidize into PdO, did not allow sufficient time for the Pd particles to be re-oxidized and redispersed. However, we cannot rule out that the low dispersion of the ballistically cooled sample is to some extent related to the exposure to moist ambient air. This interpretation would be consistent with the observations in Tables 2 and 3 for sample B aged under dry versus wet conditions. Taken together, the re-dispersion and step-wise calcination data show that the only way to maintain Pd dispersions comparable to, or greater than, those of the fresh 500 °C calcined samples is to expose the catalyst only to lean conditions and limit peak temperatures to 800 °C or less. Moreover, as shown in Table 3, absence of steam further enhances dispersions obtained under lean conditions.

The conditions that produce the highest catalyst temperatures in modern closed-loop control gasoline vehicles are hard accelerations or sustained high-power operation (such as steep hill

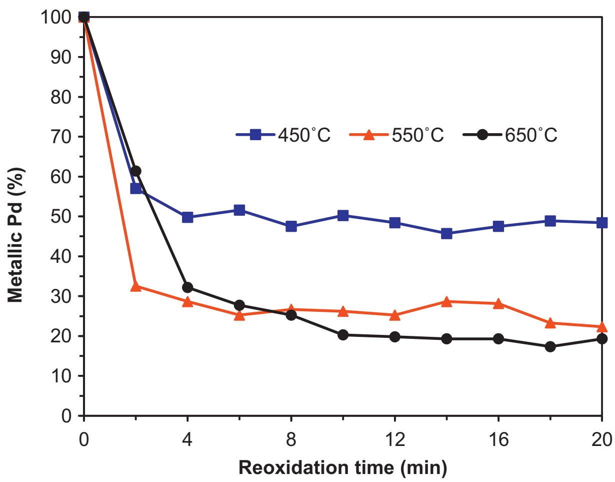

Fig. 11. Re-oxidation degree in a 10%O_2/N_2 flow of reduced 1000 °C rich-aged Pd/Al_2O_3. The experiment was measured by in situ XRD to compare the change of Pd (3 1 1) peak intensity.

climbs) that result in rich air-fuel excursions. A close-coupled TWC can achieve temperatures in excess of 800 °C under such conditions. This will inevitably occur in an exhaust gas environment containing 10% or more steam. Thus, the ideal conditions for maintaining high Pd dispersion (namely lean-only, relatively low-temperatures, absence of steam) cannot be realized in closed-loop control vehicles. Nevertheless, opportunities exist for either limiting high-temperature rich engine operation or mitigating its effects. Catalysts can be positioned downstream in the exhaust system (to limit peak temperatures), albeit with a potential cold-start emissions penalty associated with a longer warm-up time. From an air-fuel control standpoint, a common practice is to follow high-speed, high-power engine operating modes with fuel shut-off during the ensuing deceleration. This results in the engine pumping (relatively dry) air through the exhaust system, and thus offers an opportunity to re-oxidize and re-disperse the Pd particles. Although these deceleration events are typically short (less than 10 s) they take the catalyst through the temperature range where Pd re-oxidation is rapid and some measure of Pd re-dispersion may be achieved. To simulate these conditions in the laboratory, we carried out in situ XRD experiments shown in Fig. 11, in which a reduced 1000 °C rich-aged Pd/Al_2O_3 catalyst was exposed to a dry 10%O_2/N_2 flow at several temperatures spanning the range where Pd oxidation is rapid. XRD scans were taken on the fly (at 2 min intervals) following the step change in gas composition from neutral to lean. Clearly significant re-oxidation occurs during the first 2 min. While re-oxidation kinetics cannot be determined from the in situ XRD environmental chamber, the results of Fig. 11 suggest nonetheless that frequent use of deceleration fuel shut-off starting from the fresh catalyst state may be effective for arresting Pd particle growth. Additional experiments along these lines are in progress in our laboratories examining the potential for limiting Pd particle growth from the outset by restricting high-temperature rich exposure time and interspersing regenerative events such as deceleration fuel shut-off at every opportunity.

4. Conclusions

The aging of Pd/Al_2O_3 model automotive TWC catalyst components has been investigated focusing on the effects of temperature, rich or lean gas environment, and the presence or absence of steam. The Al_2O_3 support showed little degradation under the maximum temperature conditions near 1000 °C likely to be encountered in vehicle applications. Nor was there evidence that Pd underwent significant encapsulation by the support. Instead, Pd particle growth (as determined by H_2 chemisorption) was the principal mode of catalyst deactivation as reflected in increased light-off temperatures for both CO and C_3H_6 oxidation. Aging under rich conditions, in the presence of steam, and at temperatures above the PdO decomposition temperature were the main factors promoting sintering of Pd. Pd particle growth could be completely suppressed by exposing to lean conditions only at temperatures below the PdO decomposition temperature, with the highest dispersions obtained in the absence of steam. In contrast, aging under rich conditions produced much more dramatic decreases in dispersion with increasing temperature, with undetectable uptake of H_2 in some samples after 1000 °C aging. Modest re-dispersion of Pd could be achieved by re-oxidizing the high-temperature rich-aged samples. Samples that were pre-treated under oxidizing conditions showed lower CO light-off temperatures than rich pre-treated samples. While recent studies have suggested that PdO is more active than metallic Pd for CO light-off, our results suggest that Pd re-dispersion contributes to the higher CO oxidation activity of lean pre-treated samples. The conditions producing the greatest Pd particle sintering cannot be readily avoided in automotive TWC applications. However, the study also suggests ways of mitigating the extent of Pd particle sintering by decreasing peak exposure temperatures and utilizing control schemes that intermittently expose the catalyst to high temperature lean conditions.

Acknowledgements

The authors gratefully acknowledge the support from Ford URP and NSF (GOALI CBET-1159279). We thank Dr. Frank Alber (SASOL) for providing the TH100/150 alumina. The authors also acknowledge funding for the JEOL 2010F analytical electron microscope through NSF grant #DMR-9871177.

Appendix A. Supplementary data

Supplementary data associated with this article can be found, in the online version, at http://dx.doi.org/10.1016/j.apcatb.2014.08.018.

References

[1] H.S. Gandhi, G.W. Graham, R.W. McCabe, J. Catal. 216 (2003) 433.
[2] S.B. Kang, H.J. Kwon, I.-S. Nam, Y.I. Song, S.H. Oh, I&EC Res. 50 (2011) 5499–5509.
[3] H. Birgersson, M. Boutonnet, S. Järås, L. Eriksson, Topics Catal. 30/31 (2004) 1–4.
[4] I. Heo, J.W. Choung, P.S. Kim, I.-S. Nam, Y.I. Song, C.B. In, G.K. Yeo, Appl. Catal. B: Environ. 92 (2009) 114–125.
[5] G.W. Graham, H.-W. Jen, W. Chun, R.W. McCabe, J. Catal. 182 (1999) 228–233.
[6] G.W. Graham, A.E. O'Neill, A.E. Chen, Appl. Catal. A: Gen. 252 (2003) 437–445.
[7] U. Lassi, R. Polvinen, S. Suhonen, K. Kallinen, A. Savimäki, M. Härkönen, M. Valden, R.L. Keiski, Appl. Catal. A: Gen. 263 (2004) 241–248.
[8] J.C. Jiang, X.Q. Pan, G.W. Graham, R.W. McCabe, J. Schwank, Catal. Lett. 53 (1998) 37–42.
[9] J. Barbier Jr., D. Duprez, Appl. Catal. B: Environ. 4 (1994) 105–140.
[10] E. Ruckenstein, B. Pulvermacher, AIChE J. 19 (2) (1973) 356–364.
[11] E. Ruckenstein, B. Pulvermacher, J. Catal. 29 (1973) 224–245.
[12] P.C. Flynn, S.E. Wanke, J. Catal. 34 (1974) 390–399.
[13] P.C. Flynn, S.E. Wanke, J. Catal. 34 (1974) 400–410.
[14] P.C. Flynn, S.E. Wanke, J. Catal. 37 (1975) 432–448.
[15] I. Sushumna, E. Ruckenstein, J. Catal. 109 (1988) 433–462.
[16] R.M.J. Fiedorow, B.S. Chahar, S.E. Wanke, J. Catal. 51 (1978) 193–202.
[17] I. Sushumna, E. Ruckenstein, J. Catal. 109 (1987) 77–96.
[18] G.I. Straguzzi, H.R. Aduriz, C.E. Gigola, J. Catal. 66 (1980) 171–183.
[19] R.M.J. Fiedorow, S.E. Wanke, J. Catal. 43 (1976) 34–42.
[20] R. Gollob, D.B. Dadyburjor, J. Catal. 68 (1981) 473–486.
[21] D.D. Beck, C.J. Carr, J. Catal. 110 (1988) 285–297.
[22] S.A. Hassan, F.H. Khalil, F.G. El-Gamal, J. Catal. 44 (1976) 5–14.
[23] J.J. Chen, E. Ruckenstein, J. Catal. 69 (1981) 254–273.
[24] M. Hietikko, U. Lassi, K. Kallinen, A. Savimäki, M. Härkönen, J. Pursiainen, R.S. Laitinen, R.L. Keiski, Appl. Catal. A: Gen. 277 (2004) 107–117.
[25] D.L. Trimm, C.W. Lam, Chem. Eng. Sci. 35 (1980) 1405.
[26] P.O. Thevenin, E. Pocoroba, L.J. Pettersson, H. Karhu, I.J. Väyrynen, S.G. Järås, J. Catal. 207 (2002) 139–149.

[27] J.R. González-Velasco, J.A. Botas, R. Ferret, M.P. González-Marcos, J.-L. Marc, M.A. Gutiérrez-Ortiz, Catal. Today 59 (2000) 395–402.
[28] W. Zou, R.D. Gonzalez, Appl. Catal. A: Gen. 126 (1995) 351–364.
[29] H. Birgersson, M. Boutonnet, S. Järås, L. Eriksson, Top. Catal. 30/31 (2004) 433–437.
[30] N. Mousaddib, C. Feumi-Jantou, E. Garbowski, M. Primet, Appl. Catal. A: Gen. 87 (1992) 129–144.
[31] Q. Xu, K.C. Kharas, B.J. Croley, A.K. Datye, ChemCatChem 3 (2011) 1004–1014.
[32] T.W. Hansen, A.T. Delariva, S.R. Challa, A.K. Datye, Acc. Chem. Res. 46 (2013) 1720–1730.
[33] M.L. Granados, C. Larese, F.C. Galisteo, R. Mariscal, J.L.G. Fierro, R. Fernández-Ruíz, R. Sanguino, M. Luna, Catal. Today 107–108 (2005) 77–85.
[34] V. Ragaini, R. Giannantonio, P. Magni, L. Lucarelli, G. Leofanti, J. Catal. 146 (1994) 116–125.
[35] H. Zhang, J. Gromek, G.W. Fernando, S. Boorse, H.L. Marcus, J. Phase Equilib. 23 (2002) 246–248.
[36] X. Chen, J.W. Schwank, G.B. Fisher, Y. Cheng, M. Jagner, R.W. McCabe, M.B. Katz, G.W. Graham, X. Pan, Appl. Catal. A: Gen. 475 (2014) 420–426.
[37] R.J. Farrauto, M.C. Hobson, T. Kennelly, E.M. Waterman, Appl. Catal. A: Gen. 81 (1992) 227–237.
[38] S. Colussi, A. Trovarelli, E. Vesselli, A. Baraldi, G. Comelli, G. Groppi, J. Llorca, Appl. Catal. A: Gen. 390 (2010) 1–10.
[39] A. Baylet, P. Marécot, D. Duprez, P. Castellazzi, G. Groppi, P. Forzatti, Phys. Chem. Chem. Phys. 13 (2011) 4607–4613.
[40] D.R. Rainer, M. Koranne, S.M. Vesecky, D.W. Goodman, J. Phys. Chem. B 101 (1997) 10769–10774.
[41] M. Boudart, Chem. Rev. 95 (1995) 661–666.
[42] H. Lieske, J. Völter, J. Phys. Chem. 89 (1985) 1841–1842.
[43] S.-H. Oh, G.B. Hoflund, J. Phys. Chem. A 110 (2006) 7609–7613.
[44] X.-Q. Gong, Z.-P. Liu, R. Raval, P. Hu, J. Am. Chem. Soc. 126 (2004) 8–9.
[45] U.G. Singh, J. Li, J.W. Bennett, A.M. Rappe, R. Seshadri, S.L. Scott, J. Catal. 249 (2007) 349–358.
[46] K. Zorn, S. Gioegio, E. Halwax, C.R. Henry, H. Grönbeck, G. Rupprechter, J. Phys. Chem. C 115 (2011) 1103.
[47] T. Maillet, C. Solleau, J. Barbier Jr., D. Duprez, Appl. Catal. B: Environ. 14 (1997) 85–95.
[48] E.I. Altman, R.E. Tanner, Catal. Today 85 (2003) 101–111.
[49] J.F. Weaver, S.P. Devarajan, C. Hakanoglu, J. Phys. Chem. C 113 (2009) 9773–9782.
[50] J.R. Theis, R.W. McCabe, Catal. Today 184 (2012) 262–270.
[51] Y.-F.Y. Yao, J. Catal. 87 (1984) 152–162.
[52] Sh. Shaikhutdinov, M. Heemeier, M. Bäumer, T. Lear, D. Lennon, R.J. Oldman, S.D. Jackson, H.J. Freund, J. Catal. 200 (2001) 330–339.
[53] M.A. Martin, J.A. Pajares, L. Gonzales Tejuca, React. Kinet. Catal. Lett. 30 (1986) 105–111.
[54] M. Heemeier, M. Frank, J. Libuda, K. Wolter, H. Kuhlenbeck, M. Bäumer, H.-J. Freund, Catal. Lett. 68 (2000) 19–24.
[55] M.I. Zaki, G. Kunzmann, B.C. Gates, H. Knözinger, J. Phys. Chem. 91 (1987) 1486–1493.
[56] M.C. Valero, P. Raybaud, P. Sautet, Phys. Rev. B 75 (2007) 045427.